

Surface charge pattern: impact on vibrational spectroscopy and physics of charged interfaces

Wanlin Chen,[†] Marie-Pierre Gaigeot,[‡] and Simone Pezzotti*,[¶]

[†]*Department of Physical Chemistry II, Ruhr University Bochum, D-44801 Bochum, Germany*

[‡]*Université Paris-Saclay, Univ Evry, CY Cergy, LAMBE UMR8587, 91025 Evry-Courcouronnes, France ; Institut Universitaire de France (IUF), 75005 Paris, France*

[¶]*Laboratoire CPCV, Département de Chimie, École Normale Supérieure, PSL University, Sorbonne University, CNRS, 75005 Paris, France*

E-mail: simone.pezzotti@ens.psl.eu

Abstract

Surface-specific vibrational spectroscopies revolutionized the study of charged interfaces, by sensitively probing water's response in the electric double layer (EDL) and correlating it with surface charge via models like Gouy-Chapman-Stern. The assumed one-to-one relationship between water's spectroscopic response and surface charge has been widely accepted without question. We hereby propose a theoretical experiment to evaluate this assumption. Interestingly, our findings reveal a non one-to-one relationship between surface charge and spectroscopic response, exhibiting a fascinating dependence on surface topology.

What is the protonation state of an oxide surface in contact with liquid water? What is the point of zero charge of an electrode-electrolyte interface? How do ions (and water) arrange and screen the electric field within the electric double layer (EDL)? Despite more than a century of intensive research, these fundamental questions in interface science remain challenging to address, both in theory and experiments.¹⁻¹⁰ In the last decades, surface specific spectroscopies, such as vibrational Sum Frequency Generation (vSFG) and Second Harmonic Generation (SHG), opened a possibility of gaining insights by sensitively probing the response of water within the EDL.^{1-3,10-31} This response is often used to deduce the surface charge (σ), via a commonly assumed one-to-one correspondence based on the Gouy-Chapman-Stern (GCS) model and its derivations.^{13-15,18,21,25,26,31}

SFG and SHG experiments probe the second order susceptibility, $\chi^{(2)}$, which is interface-specific since $\chi^{(2)} \neq 0$ only for non-centrosymmetric media, e.g. aqueous interfaces, while $\chi^{(2)} = 0$ in the centrosymmetric bulk.³²⁻³⁴ The $\chi^{(2)}$ response from a charged interface is given by the sum of two contributions respectively arising from the topmost Binding Interfacial Layer (BIL, where the molecular organization and H-bond network substantially differ from bulk aqueous solutions due to the direct contact with the surface and ions adsorption), and from the subsequent diffuse layer (DL, composed by bulk-like water oriented by the surface electric field and by dissolved mobile ions):^{1-3,10,14,16,18,25,27-29,35}

$$\chi^{(2)}(\omega) = \chi_{BIL}^{(2)}(\omega) + \chi_{DL}^{(2)} \quad (1)$$

$\chi_{DL}^{(2)}(\omega)$ contains the response of water within the EDL. Nowadays, several approaches have been devised to extract $\chi_{DL}^{(2)}(\omega)$ from the measured $\chi^{(2)}(\omega)$,^{1-3,14,16,25,35} and most recently techniques that are specifically sensitive to $\chi_{DL}^{(2)}(\omega)$, such as phase resolved SHG, have been developed.^{18,31} As remarked in many studies, $\chi_{DL}^{(2)}(\omega)$ can be expressed as:

$$\chi_{DL}^{(2)}(\omega) = \chi_{Bulk}^{(3)}(\omega) \int_{z_a}^{\infty} dz \cdot E_{DC}(z) e^{i\Delta k_z z} \quad (2)$$

where $E_{\text{DC}}(z)$ is the electric field profile along the z-direction perpendicular to the surface and Δk_z is a phase factor that takes into account interferences between the emitted light at different depths from the surface.^{14,15,21,24,25,35} The integral runs across the EDL region, with z_a being the boundary between BIL and DL. $\chi_{\text{Bulk}}^{(3)}(\omega)$ is the bulk water third order susceptibility.^{14,25} The surface charge, σ , is usually determined by using GCS to approximate the $E_{\text{DC}}(z)$ dependence on z . The prerequisite of this model is that, at fixed electrolyte composition, the same σ must always result in the same $\chi_{\text{DL}}^{(2)}(\omega)$.

Since the seminal work from Eienthal and coworkers,¹³ this approach has been widely employed to perform SHG and SFG spectroscopic titration for oxide surfaces in contact with aqueous solutions of varying pH,^{2,13,16,36-39} to study the way electrolyte solutions screen the surface field,^{1-3,14,17,27,28,31,35,40-42} to determine the charge state of the surface and the solution response in electrochemistry,^{10-12,30,43-46} to probe charge separation and recombination during interfacial chemical reactions,⁴⁷⁻⁴⁹ to cite a few. Each of these studies substantially advanced our understanding of the complex chemico-physical properties of charged aqueous interfaces. However, despite being at the heart of this emerging research field, the assumption that one and only one $\chi_{\text{DL}}^{(2)}(\omega)$ corresponds to one given σ value (for fixed electrolyte composition) has never been assessed so far. One reason is that such an assumption is implicitly encoded into our textbook understanding of the EDL response to the electric field.

Hereafter, we test this hypothesis with a theoretical experiment, by means of classical molecular dynamics (MD) of the minimal required complexity. We used the LAMMPS⁵⁰ code to simulate a 35 mM NaCl aqueous solution between identical charged walls (fig. 1-A). To keep the model as simple as possible, the walls are built to represent a generic weakly interacting surface, with the interaction parameters introduced by Huang et al.^{51,52} The ions concentration is kept intentionally low to ensure that we are on the range of validity of GCS, while being high enough to avoid unwanted interference effects in the $\chi^2(\omega)$.¹⁵ The surface charge is implemented in two ways: (i) a homogeneous distribution among all topmost wall atoms; (ii) a heterogeneously distributed surface charge, randomly assigned to only some

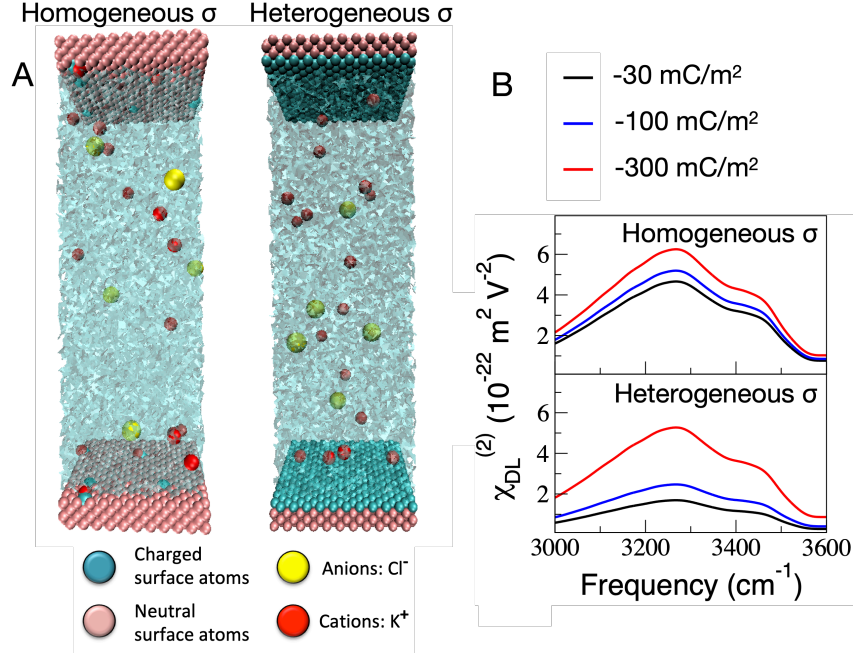


Figure 1: Theoretical experiment challenging the commonly assumed one-to-one correspondence between $\chi_{DL}^{(2)}(\omega)$ and σ . (A) MD-snapshots illustrating the model interfaces with homogeneous and heterogeneous σ patterns (for $\sigma = -100 \text{ mC/m}^2$ as an example). (B) $\text{Im}\chi_{DL}^{(2)}(\omega)$ spectra computed from six MD simulations. The intensity is markedly different for heterogeneous *vs* homogeneous surface charge distributions: σ cannot be deduced from $\chi_{DL}^{(2)}(\omega)$ without knowing the surface pattern.

of the topmost atoms. A total of six model systems were considered, with $\sigma = -30, -100, -300 \text{ mC/m}^2$, covering the typical surface charge of silica/water interfaces in the 2-14 pH range.^{4,16,27,41} Indeed, most SFG/SHG titration studies have been performed on silica/water interfaces,^{2,13,16,36-38} where SiOH terminations and therefore surface charge patterns can be more or less heterogeneous depending on the way the surface is pre-treated.⁵³⁻⁵⁵ These studies, such as those by Gibbs *et al.*^{3,37,38} and many others,⁵⁶ have yielded some of the most intriguing yet controversial results in the field of interface spectroscopy, revealing a still-unexplained dependence of the spectroscopic response on surface preparation methods.

We computed theoretical SFG $\text{Im}\chi_{DL}^{(2)}(\omega)$ spectra for all systems (see the method section for all details). Based on the current state of knowledge, we expect the $\text{Im}\chi_{DL}^{(2)}(\omega)$ spectrum to be identical for model interfaces with the same surface charge σ , regardless of whether the

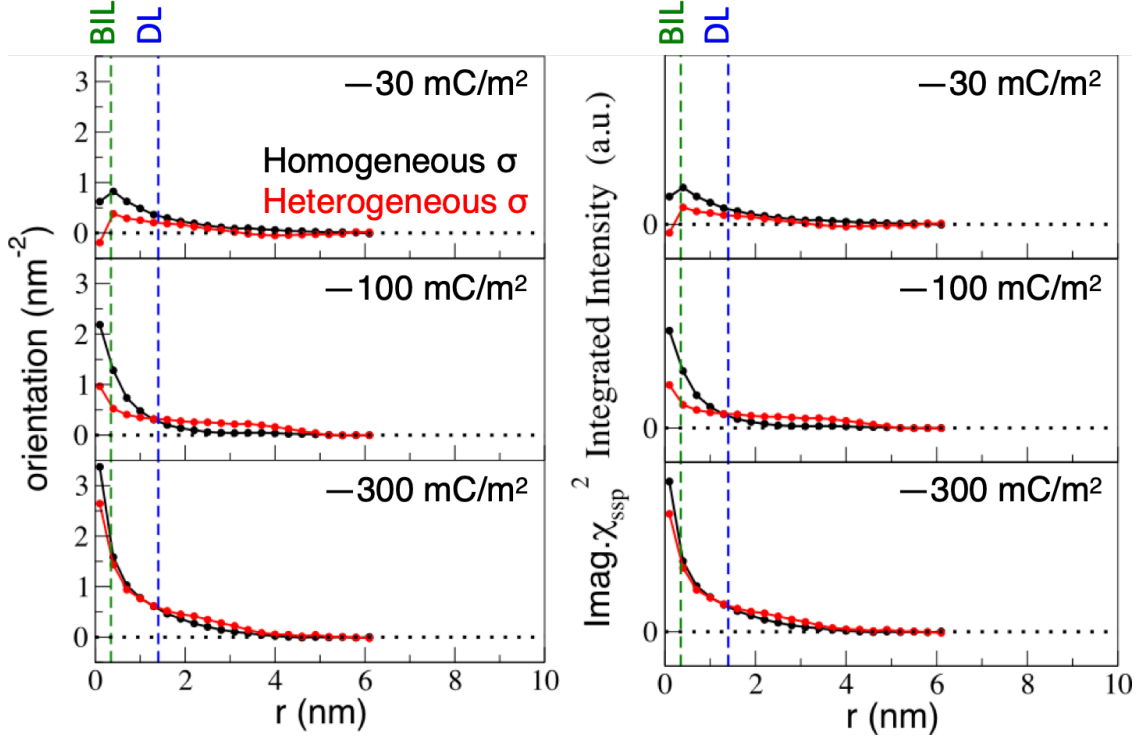


Figure 2: Surface pattern influences the electrolyte response in the DL (diffuse layer). (A) Water orientation profile ($\sum_{i=1}^{N_W} \cos\theta_i$ normalized by surface area, see eq.4 in the method section) along r - the vertical distance from the surface. (B) Corresponding r -profiles for $\text{Im}\chi_{DL}^{(2)}(\omega)$ intensity (integrated over 3000-3600 cm^{-1}), as computed from $\sum_{i=1}^{N_W} \cos\theta_i$ with eq.4 (method section). The vertical green dashed line marks the boundary between BIL and DL regions. The blue dashed line marks a plane located 1 nm within the DL.

charge distribution is heterogeneous or homogeneous. However, this is not what we observe in Fig.1-B.

While all spectra exhibit the expected two-band structure of the $\text{Im}\chi_{DL}^{(2)}(\omega)$ (with maxima at ~ 3200 and 3400 cm^{-1}),^{14,24,25} the intensity is strikingly higher (by up to three times) for homogeneously charged surfaces than for their heterogeneous counterparts. The difference is most marked for DL for the lowest σ , and slowly decreases - but persists - with increasing charging. The molecular origin of this effect lies in the sensitivity of the field-induced water alignment to the surface charge patterning, as shown in fig.2-left by means of water orientation profiles. These are particularly informative since the net water orientation in the DL region is directly proportional to the intensity of $\chi_{DL}^{(2)}$ (eq.4 in the method section), as shown in fig.2-right.

All orientation profiles show the expected decay after the boundary between BIL and DL (green dashed line); the magnitude is, however, different from case to case and follows the trend observed in the topmost interfacial BIL layer. The orientational response of BIL water (before the green dashed line) substantially differs depending on the way the surface is charged: BIL (as well as the subsequent DL) water is systematically more efficiently aligned by the homogeneous rather than by the heterogeneous surface charge distributions (black *vs.* red in the plot). This difference should not be regarded as surprising since many recent studies, both theoretical and experimental, have demonstrated how sensitive the arrangement of hydration water is to the way the polar/charged groups are distributed over the surface.^{57–65} This is because the water response does not depend on single water-surface interactions, but on the collective rearrangement of the water H-bond network in response to the local distribution of polar groups at the surface.^{57,60–63,65} In particular, studies on the wetting of patterned surfaces have shown that the surface is most wet, and accordingly, the water H-bond network is most perturbed, when the polar groups are dispersed as homogeneously as possible over the surface, while the effect is minimized when the polar groups are clustered over a few small surface areas.⁶¹ The same reasoning can be applied here to explain why BIL and DL water molecules are best aligned by the homogeneous charge distributions.

In conclusion, the result of our theoretical experiment challenges the commonly assumed one-to-one correspondence between the surface charge and the electrolyte response to the electric field at the interface, as measured by $\chi_{DL}^{(2)}(\omega)$: indeed, we showed that the same σ value can result in significantly different $\chi_{DL}^{(2)}$ responses depending on the specific distribution of charge across the surface. This insight may help explain the unresolved findings from the past 30 years of SFG/SHG titration studies on silica/water interfaces, where variations in surface charge patterning (i.e., the distribution of SiOH terminations) likely arose due to differences in surface preparation across studies.^{3,37,38,53–55} Our findings indicate that such charge patterning results in significantly different SFG/SHG intensities, as a function of pH.

More generally, our results also demonstrate that the electrolyte screening within the EDL

is a 3-Dimensional (3D) problem, sensitive to the lateral charge distribution over the surface together with the specific properties of the interfacial water H-bond network. This calls for further developments of EDL theories, beyond commonly adopted 1D models (e.g., GCS and its derivatives), where surface topology and molecular interactions should be explicitly included, in line with most recent insights from MD simulation studies.⁶⁶ We also stress the importance of independently measuring surface charge and $\chi_{DL}^{(2)}(\omega)$ to fully exploit the exciting perspectives offered by SFG and SHG spectroscopies in interface science. This is nowadays possible thanks to emerging techniques, such as the experimental scheme recently introduced by Liu and coworkers for in situ SFG spectroscopy of oxide surfaces in liquid water.^{4,67}

We believe that combining SFG and SHG probes of DL water with these approaches, along with advanced theoretical molecular-level 3D EDL models,⁶⁶ will pave the way for a deeper understanding of the complex relationships between surface topology, interfacial water networks, ion distributions, and electric fields at solid-liquid interfaces.

Methods

For all simulations, the water+NaCl system was described using the force field developed by Kann and Skinner,⁶⁸ with TIP4P/2005 water and rescaled (by 0.85) ions charge. Charge rescaling effectively describes ion polarisability.⁶⁸ Lorentz-Berthelot mixing rules were adopted for wall-electrolyte interactions. We systematically considered $[\text{NaCl}] = 35 \text{ mM}$ and added the appropriate number of sodium counter-ions to generate neutral simulation boxes, in a liquid phase of 11465 water molecule (held rigid using the SHAKE algorithm). To impose a pressure of 1 atm, we used the top wall as a piston until an equilibrium height was reached, leading to box xy-dimensions of 48.2 Å and a vertical z-dimension of 267 Å. Subsequent equilibration and production runs were of 32 ns each (NVT ensemble, T= 298 K, Nosé-Hoover thermostat⁶⁹).

Theoretical SFG spectra were computed following the procedure of ref. ⁷⁰ In short, $\chi_{DL}^{(2)}(\omega)$ is expressed by the Fourier transform of the dipole (μ)-polarizability (α) correlation function, ⁷¹ by considering all the cross-correlation terms between the N_{DL} water molecules located in the DL layer and all the N_W water molecules of the simulated system:

$$\chi_{DL}^{(2)}(\omega) = \frac{i\omega}{k_B T} \sum_{i=1}^{N_{DL}} \left(\sum_{j=1}^{N_W} \int_0^\infty dt e^{i\omega t} \langle \alpha_{xx}^j(t) \mu_z^i(0) \rangle \right) = \sum_{i=1}^{N_{DL}} \beta_{DL}^i(\omega) \quad (3)$$

where $\beta_{DL}^i(\omega) = \frac{i\omega}{k_B T} \sum_{j=1}^{N_W} \int_0^\infty dt \exp(i\omega t) \langle \alpha_{xx}^j(t) \mu_z^i(0) \rangle$ is the contribution of the i -th DL-water molecule. The SFG activity of DL-water is dominated by the dipole orientation of the water molecules, ^{14,24,25} which hence leads to $\chi_{DL}^{(2)}(\omega)$ being calculated via the following equation: ⁷⁰

$$\chi_{DL}^{(2)}(\omega) = \sum_{i=1}^{N_{DL}} \frac{\beta_{DL}^i(\omega)}{\cos\theta_i} \cdot \cos\theta_i \quad (4)$$

where the orientational term (with θ_i being the angle formed between the dipole of the i -th water molecule and the normal to the surface) is directly obtained from the MD simulations, while $\frac{\beta_{DL}^i(\omega)}{\cos\theta_i}$ has been parameterized in ref. ⁷⁰.

Acknowledgement

S. P. acknowledges funding from the European Research Council (ERC, ELECTROPHOBIC, Grant Agreement No. 101077129). W.C. acknowledges the Alexander von Humboldt Foundation (AvH) for the research fellowship under the Henriette-Hertz-Scouting Program. Simulations were conducted using HPC resources from GENCI-France under Grant 072484 (CINES/IDRIS/TGCC). We acknowledge Prof. L. Joly and Dr. Fu Li, as well as Prof. Y. Ron Shen and Prof. Weitao Liu for fruitful discussions.

References

- (1) Gonella, G.; Backus, E. H.; Nagata, Y.; Bonthuis, D. J.; Loche, P.; Schlaich, A.; Netz, R. R.; Kühnle, A.; McCrum, I. T.; Koper, M. T. M.; others. Water at charged interfaces. *Nat. Rev. Chem.* **2021**, *5*, 466–485
- (2) Bañuelos, J. L.; Borguet, E.; Brown Jr, G. E.; Cygan, R. T.; DeYoreo, J. J.; Dove, P. M.; Gaignot, M.-P.; Geiger, F. M.; Gibbs, J. M.; Grassian, V. H.; others. Oxide–and silicate–water interfaces and their roles in technology and the environment. *Chem. Rev.* **2023**, *123*, 6413–6544
- (3) Rehl, B.; Ma, E.; Parshotam, S.; DeWalt-Kerian, E. L.; Liu, T.; Geiger, F. M.; Gibbs, J. M. Water structure in the electrical double layer and the contributions to the total interfacial potential at different surface charge densities. *J. Am. Chem. Soc.* **2022**, *144*, 16338–16349
- (4) Li, X.; Brigiano, F. S.; Pezzotti, S.; Liu, X.; Chen, W.; Chen, H.; Li, Y.; Li, H.; Lin, X.; Zheng, W.; others. Unconventional structural evolution of an oxide surface in water unveiled by in situ sum-frequency spectroscopy. *Nat. Chem.* **2025**, *17*, 198–203
- (5) Ojha, K.; Arulmozhi, N.; Aranzales, D.; Koper, M. T. Double layer at the Pt (111)–aqueous electrolyte interface: potential of zero charge and anomalous Gouy–Chapman screening. *Angew. Chem. Int. Ed.* **2020**, *132*, 721–725
- (6) Levell, Z.; Le, J.; Yu, S.; Wang, R.; Ethirajan, S.; Rana, R.; Kulkarni, A.; Resasco, J.; Lu, D.; Cheng, J.; others. Emerging Atomistic Modeling Methods for Heterogeneous Electrocatalysis. *Chem. Rev.* **2024**, *124*, 8620–8656
- (7) Groß, A.; Sakong, S. Ab initio simulations of water/metal interfaces. *Chem. Rev.* **2022**, *122*, 10746–10776

- (8) Ringe, S.; Hormann, N. G.; Oberhofer, H.; Reuter, K. Implicit solvation methods for catalysis at electrified interfaces. *Chem. Rev.* **2021**, *122*, 10777–10820
- (9) Wu, J. Understanding the electric double-layer structure, capacitance, and charging dynamics. *Chem. Rev.* **2022**, *122*, 10821–10859
- (10) Gardner, A. M.; Saeed, K. H.; Cowan, A. J. Vibrational sum-frequency generation spectroscopy of electrode surfaces: studying the mechanisms of sustainable fuel generation and utilisation. *Phys. Chem. Chem. Phys.* **2019**, *21*, 12067–12086
- (11) Speelman, R.; Marker, E. J.; Geiger, F. M. Quantifying Stern layer water alignment before and during the oxygen evolution reaction. *Sci. Adv.* **2025**, *11*, eado8536
- (12) Xu, P.; von Rueden, A. D.; Schimmenti, R.; Mavrikakis, M.; Suntivich, J. Optical method for quantifying the potential of zero charge at the platinum–water electrochemical interface. *Nat. Mater.* **2023**, *22*, 503–510
- (13) Ong, S.; Zhao, X.; Eienthal, K. B. Polarization of water molecules at a charged interface: second harmonic studies of the silica/water interface. *Chem. Phys. Lett.* **1992**, *191*, 327–335
- (14) Wen, Y.-C.; Zha, S.; Liu, X.; Yang, S.; Guo, P.; Shi, G.; Fang, H.; Shen, Y. R.; Tian, C. Unveiling microscopic structures of charged water interfaces by surface-specific vibrational spectroscopy. *Phys. Rev. Lett.* **2016**, *116*, 016101
- (15) Gonella, G.; Lutgebaucks, C.; de Beer, A. G. F.; Roke, S. Second Harmonic and Sum-Frequency Generation from Aqueous Interfaces Is Modulated by Interference. *J. Phys. Chem. C.* **2016**, *120*, 9165–9173
- (16) Wei, F.; Urashima, S.-h.; Nihonyanagi, S.; Tahara, T. Elucidation of the pH-dependent electric double layer structure at the silica/water interface using heterodyne-detected

- vibrational sum frequency generation spectroscopy. *J. Am. Chem. Soc.* **2023**, *145*, 8833–8846
- (17) Dalstein, L.; Chiang, K.-Y.; Wen, Y.-C. Surface Potential at Electrolyte/Air Interfaces: A Quantitative Analysis via Sum-Frequency Vibrational Spectroscopy. *J. Phys. Chem. B* **2023**, *127*, 4915–4921
- (18) Dalstein, L.; Chiang, K.-Y.; Wen, Y.-C. Direct quantification of water surface charge by phase-sensitive second harmonic spectroscopy. *J. Phys. Chem. Lett.* **2019**, *10*, 5200–5205
- (19) Uddin, M. M.; Azam, M. S.; Hore, D. K. Variable-Angle Surface Spectroscopy Reveals the Water Structure in the Stern Layer at Charged Aqueous Interfaces. *J. Am. Chem. Soc.* **2024**, *146*, 11756–11763
- (20) Rehl, B.; Gibbs, J. M. Role of ions on the surface-bound water structure at the silica/water interface: Identifying the spectral signature of stability. *J. Phys. Chem. Lett.* **2021**, *12*, 2854–2864
- (21) Ohno, P. E.; Saslow, S. A.; fei Wang, H.; Geiger, F. M.; Eisenthal, K. B. Phase-referenced nonlinear Spectroscopy of the alpha-quartz/water Interface. *Nat. Comm.* **2016**, *7*, 13587–13591
- (22) Geiger, F. M. Second harmonic generation, sum frequency generation, and χ (3): dissecting environmental interfaces with a nonlinear optical Swiss Army knife. *Annu. Rev. Phys. Chem.* **2009**, *60*, 61–83
- (23) Chu, B.; Roke, S.; Marchioro, A. Does the ionic distribution in the electrical double layer modify second harmonic scattering? *J. Chem. Phys.* **2024**, *160*
- (24) Joutsuka, T.; Hirano, T.; Sprik, M.; Morita, A. Effects of third-order susceptibility in

- sum frequency generation spectra: a molecular dynamics study in liquid water. *Phys. Chem. Chem. Phys.* **2018**, *20*, 3040–3053
- (25) Pezzotti, S.; Galimberti, D. R.; Shen, Y. R.; Gaigeot, M.-P. Structural definition of the BIL and DL: a new universal methodology to rationalize non-linear $\chi^{(2)}$ (ω) SFG signals at charged interfaces, including $\chi^{(3)}$ (ω) contributions. *Phys. Chem. Chem. Phys.* **2018**, *20*, 5190–5199
- (26) Pezzotti, S.; Galimberti, D. R.; Shen, Y. R.; Gaigeot, M.-P. What the diffuse layer (DL) reveals in non-linear SFG spectroscopy. *Minerals* **2018**, *8*, 305
- (27) Tuladhar, A.; Dewan, S.; Pezzotti, S.; Brigiano, F. S.; Creazzo, F.; Gaigeot, M.-P.; Borguet, E. Ions tune interfacial water structure and modulate hydrophobic interactions at silica surfaces. *J. Am. Chem. Soc.* **2020**, *142*, 6991–7000
- (28) Chen, W.; Sanders, S. E.; Ozdamar, B.; Louaas, D.; Brigiano, F. S.; Pezzotti, S.; Petersen, P. B.; Gaigeot, M.-P. On the trail of molecular hydrophilicity and hydrophobicity at aqueous interfaces. *J. Phys. Chem. Lett.* **2023**, *14*, 1301–1309
- (29) Hore, D. K.; Tyrode, E. Probing charged aqueous interfaces near critical angles: effect of varying coherence length. *J. Phys. Chem. C* **2019**, *123*, 16911–16920
- (30) Wang, H.; Xu, Q.; Liu, Z.; Tang, Y.; Wei, G.; Shen, Y. R.; Liu, W.-T. Gate-controlled sum-frequency vibrational spectroscopy for probing charged oxide/water interfaces. *J. Phys. Chem. Lett.* **2019**, *10*, 5943–5948
- (31) Ohno, P. E.; Chang, H.; Spencer, A. P.; Liu, Y.; Boamah, M. D.; Wang, H.-f.; Geiger, F. M. Beyond the Gouy–Chapman model with heterodyne-detected second harmonic generation. *J. Phys. Chem. Lett.* **2019**, *10*, 2328–2334
- (32) Du, Q.; Freysz, E.; Shen, Y. R. Vibrational spectra of water molecules at quartz/water interfaces. *Phys. Rev. Lett.* **1994**, *72*, 238

- (33) Ostroverkhov, V.; Waychunas, G. A.; Shen, Y. R. New information on water interfacial structure revealed by phase-sensitive surface spectroscopy. *Phys. Rev. Lett.* **2005**, *94*, 046102
- (34) Ji, N.; Ostroverkhov, V.; Tian, C. S.; Shen, Y. R. Characterization of Vibrational Resonances of Water-Vapor Interfaces by Phase-Sensitive Sum-Frequency Spectroscopy. *Phys. Rev. Lett.* **2008**, *100*, 096102
- (35) Backus, E. H. G.; Schaefer, J.; Bonn, M. Probing the mineral–water interface with nonlinear optical spectroscopy. *Angew. Chem. Int. Ed.* **2021**, *60*, 10482–10501
- (36) Azam, M. S.; Weeraman, C. N.; Gibbs-Davis, J. M. Specific cation effects on the bimodal acid–base behavior of the silica/water interface. *J. Phys. Chem. Lett.* **2012**, *3*, 1269–1274
- (37) Darlington, A. M.; Gibbs-Davis, J. M. Bimodal or trimodal? The influence of starting pH on site identity and distribution at the low salt aqueous/silica interface. *J. Phys. Chem. C* **2015**, *119*, 16560–16567
- (38) Azam, M. S.; Weeraman, C. N.; Gibbs-Davis, J. M. Halide-induced cooperative acid–base behavior at a negatively charged interface. *J. Phys. Chem. C* **2013**, *117*, 8840–8850
- (39) Sung, J.; Shen, Y. R.; Waychunas, G. A. The interfacial structure of water/protonated α -Al₂O₃ (1120) as a function of pH. *J. Phys. Condens. Matter* **2012**, *24*, 124101
- (40) Covert, P. A.; Jena, K. C.; Hore, D. K. Throwing salt into the mix: Altering interfacial water structure by electrolyte addition. *J. Phys. Chem. Lett.* **2014**, *5*, 143–148
- (41) Pezzotti, S.; Galimberti, D. R.; Gaigeot, M.-P. Deconvolution of BIL-SFG and DL-SFG spectroscopic signals reveals order/disorder of water at the elusive aqueous silica interface. *Phys. Chem. Chem. Phys.* **2019**, *21*, 22188–22202

- (42) Hunger, J.; Schaefer, J.; Ober, P.; Seki, T.; Wang, Y.; Prädell, L.; Nagata, Y.; Bonn, M.; Bonthuis, D. J.; Backus, E. H. G. Nature of cations critically affects water at the negatively charged silica interface. *J. Am. Chem. Soc.* **2022**, *144*, 19726–19738
- (43) Montenegro, A.; Dutta, C.; Mammetkuliev, M.; Shi, H.; Hou, B.; Bhattacharyya, D.; Zhao, B.; Cronin, S. B.; Benderskii, A. V. Asymmetric response of interfacial water to applied electric fields. *Nature* **2021**, *594*, 62–65
- (44) Zhang, Y.; de Aguiar, H. B.; Hynes, J. T.; Laage, D. Water structure, dynamics, and sum-frequency generation spectra at electrified graphene interfaces. *J. Phys. Chem. Lett.* **2020**, *11*, 624–631
- (45) Liu, W.-T.; Shen, Y. R. In situ sum-frequency vibrational spectroscopy of electrochemical interfaces with surface plasmon resonance. *Proc. Natl. Acad. Sci.* **2014**, *111*, 1293–1297
- (46) Liu, Z.; Li, Y.; Xu, Q.; Wang, H.; Liu, W.-T. Coherent vibrational spectroscopy of electrochemical interfaces with plasmonic nanogratings. *J. Phys. Chem. Lett.* **2019**, *11*, 243–248
- (47) Matsuzaki, K.; Kusaka, R.; Nihonyanagi, S.; Yamaguchi, S.; Nagata, T.; Tahara, T. Partially hydrated electrons at the air/water interface observed by UV-excited time-resolved heterodyne-detected vibrational sum frequency generation spectroscopy. *J. Am. Chem. Soc.* **2016**, *138*, 7551–7557
- (48) Saak, C.-M.; Backus, E. H. G. The Role of Sum-Frequency Generation Spectroscopy in Understanding On-Surface Reactions and Dynamics in Atmospheric Model-Systems. *J. Phys. Chem. Lett.* **2024**, *15*, 4546–4559
- (49) Backus, E. H. G.; Hosseinpour, S.; Ramanan, C.; Sun, S.; Schlegel, S. J.; Zelenka, M.; Jia, X.; Gebhard, M.; Devi, A.; Wang, H. I.; others. Ultrafast Surface-Specific Spec-

- troscopy of Water at a Photoexcited TiO₂ Model Water-Splitting Photocatalyst. *Angew. Chem. Int. Ed.* **2024**, *63*, e202312123
- (50) Plimpton, S. Fast parallel algorithms for short-range molecular dynamics. *J. Chem. Phys.* **1995**, *117*, 1–19
- (51) Huang, D.; Cottin-Bizonne, C.; Ybert, C.; Bocquet, L. Ion-Specific Anomalous Electrokinetic Effects in Hydrophobic Nanochannels. *Phys. Rev. Lett.* **2007**, *98*, 177801
- (52) Huang, D. M.; Cottin-Bizonne, C.; Ybert, C.; Bocquet, L. Aqueous Electrolytes near Hydrophobic Surfaces: Dynamic Effects of Ion Specificity and Hydrodynamic Slip. *Langmuir* **2008**, *24*, 1442–1450
- (53) Rimola, A.; Costa, D.; Sodupe, M.; Lambert, J.-F.; Ugliengo, P. Silica surface features and their role in the adsorption of biomolecules: computational modeling and experiments. *Chem. Rev.* **2013**, *113*, 4216–4313
- (54) Cyran, J. D.; Donovan, M. A.; Vollmer, D.; Brigiano, F. S.; Pezzotti, S.; Galimberti, D. R.; Gageot, M.-P.; Bonn, M.; Backus, E. H. G. Molecular hydrophobicity at a macroscopically hydrophilic surface. *Proc. Natl. Acad. Sci.* **2019**, *116*, 1520–1525
- (55) Dalstein, L.; Potapova, E.; Tyrode, E. The elusive silica/water interface: Isolated silanols under water as revealed by vibrational sum frequency spectroscopy. *Phys. Chem. Chem. Phys.* **2017**, *19*, 10343–10349
- (56) Bañuelos, J. L.; Borguet, E.; Brown Jr, G. E.; Cygan, R. T.; DeYoreo, J. J.; Dove, P. M.; Gageot, M.-P.; Geiger, F. M.; Gibbs, J. M.; Grassian, V. H.; others. Oxide–and silicate–water interfaces and their roles in technology and the environment. *Chem. Rev.* **2023**, *123*, 6413–6544
- (57) Rego, N. B.; Patel, A. J. Understanding hydrophobic effects: Insights from water density fluctuations. *Annu. Rev. Condens. Matter Phys.* **2022**, *13*, 303–324

- (58) Giovambattista, N.; DeBenedetti, P. G.; Rosky, P. J. Hydration behavior under confinement by nanoscale surfaces with patterned hydrophobicity and hydrophilicity. *J. Phys. Chem. C* **2007**, *111*, 1323–1332
- (59) Lee, C.-Y.; McCammon, J. A.; Rosky, P. The structure of liquid water at an extended hydrophobic surface. *J. Chem. Phys.* **1984**, *80*, 4448–4455
- (60) Xi, E.; Venkateshwaran, V.; Li, L.; Rego, N.; Patel, A. J.; Garde, S. Hydrophobicity of proteins and nanostructured solutes is governed by topographical and chemical context. *Proc. Natl. Acad. Sci.* **2017**, *114*, 13345–13350
- (61) Rego, N. B.; Ferguson, A. L.; Patel, A. J. Learning the relationship between nanoscale chemical patterning and hydrophobicity. *Proc. Natl. Acad. Sci.* **2022**, *119*, e2200018119
- (62) Wang, R.; DelloStritto, M.; Klein, M. L.; Borguet, E.; Carnevale, V. Topological properties of interfacial hydrogen bond networks. *Phys. Rev. B* **2024**, *110*, 014105
- (63) Monroe, J.; Barry, M.; DeStefano, A.; Gokturk, P. A.; Jiao, S.; Robinson-Brown, D.; Webber, T.; Crumlin, E. J.; Han, S.; Shell, M. S. Water Structure and Properties at Hydrophilic and Hydrophobic Surfaces. *Annu. Rev. Chem. Biomol.* **2020**, *11*, 523–557
- (64) Jiao, S.; Shell, M. S. Inverse design of pore wall chemistry and topology through active learning of surface group interactions. *J. Chem. Phys.* **2024**, *160*
- (65) Adams, E. M.; Pezzotti, S.; Ahlers, J.; Rüttermann, M.; Levin, M.; Goldenzweig, A.; Peleg, Y.; Fleishman, S. J.; Sagi, I.; Havenith, M. Local Mutations Can Serve as a Game Changer for Global Protein Solvent Interaction. *JACS Au* **2021**, *1*, 1076–1085
- (66) Nauman, J. A.; Suvlu, D.; Willard, A. P. Electric Fields at Solid-Liquid Interfaces: Insights from Molecular Dynamics Simulation. *Annu. Rev. Phys. Chem.* **2024**, *76*
- (67) Liu, W.-T.; Shen, Y. R. Sum-frequency phonon spectroscopy on α -quartz. *Phys. Rev. B Condens. Matter* **2008**, *78*, 024302

- (68) Kann, Z. R.; Skinner, J. L. A scaled-ionic-charge simulation model that reproduces enhanced and suppressed water diffusion in aqueous salt solutions. *J. Chem. Phys.* **2014**, *141*, 104507
- (69) Hoover, W. G. Canonical dynamics: Equilibrium phase-space distributions. *Phys. Rev. A* **1985**, *31*, 1695–1697
- (70) Chen, W.; Louaas, D.; Brigiano, F. S.; Pezzotti, S.; Gaigeot, M.-P. A simplified method for theoretical sum frequency generation spectroscopy calculation and interpretation: The “pop model”. *J. Chem. Phys.* **2024**, *161*, 144115
- (71) Morita, A.; Hynes, J. T. A Theoretical Analysis of the SFG Spectrum of the Water Surface. II- Time Dependent Approach. *J. Phys. Chem. B.* **2002**, *106*, 673–685